



# Integral Sliding Mode Control for Antiskid Braking System of Unmanned Aerial Vehicles Based on Extended State Observer

Mingjun Xie<sup>1</sup>, Yuhong Jia<sup>2</sup>(✉), and Song Ding<sup>3</sup>

<sup>1</sup> Large Aircraft Advanced Training Center, Beihang University, Beijing 100083, China

<sup>2</sup> School of Aeronautic Science and Engineering, Beihang University, Beijing 100083, China  
jia.yuhong@buaa.edu.cn

<sup>3</sup> Ningbo Institute of Technology, Beihang University, Ningbo 315800, China

**Abstract.** This article addresses an integral sliding mode control (ISMC) method for antiskid braking system (ABS) of unmanned aerial vehicles (UAV) based on extended state observer (ESO) to track the real-time optimal slip ratio. First, based on reasonable simplification, a comprehensive dynamic model of the UAV braking system is established. Then, an ESO is designed to guarantee the precise estimation of uncertainty disturbance during aircraft ground taxiing, an ABS controller is generated by combining ISMC and ESO. Finally, simulation is carried out under different working conditions, including representative road, step reduction of braking torque, road changed suddenly, and parameter high-low bias. The simulation results verify the effectiveness of the proposed slip ratio control strategy.

**Keywords:** Antiskid braking system · Slip ratio · Extended state observer · Integral sliding mode control

## 1 Introduction

Ground taxiing is a critical stage in the safe take-off and landing of UAV, and efficient ABS control strategy plays a vital role in ground taxiing [1]. Compared with the traditional wheel deceleration control strategy, the sliding ratio control strategy has been regarded as a better ABS control strategy [2]. The essence of slip rate control is that the actual slip ratio tracks its optimal value, so as to obtain the maximum adhesive coefficient.

Various control algorithms have been proposed to track the optimal slip ratio, such as PID control [3], backstepping control [4], fuzzy control [5], neural network control [6], and model predictive control [7] etc. Although the above methods can improve the ground taxiing performance of UAV in a certain extent, there are still problems such as high accuracy requirements for the system model and weak adaptability of the perturbation parameters. Besides, it is generally assumed that the optimal slip ratio is a constant value, but in fact it is susceptible to runway status and UAV speed. The optimal slip rate of UAV is constantly changing when it is taxiing on the ground.

ESO proposed by Han [8] can not only observe the state of the system, but also observe the uncertainty factors of the system. It extends the total disturbance of the model uncertainty part and the external disturbance into the state variables of the system, and can estimate the total disturbance. ISMC eliminates process of sliding mode control from the initial state to the sliding surface, and retains the advantages of sliding mode control converging to the target value in a finite time [9]. With the purpose of tracking the real-time optimal slip ratio, this article proposes an ISMC method based on ESO, which combines the advantages of ESO and ISMC.

## 2 Mathematical Model of ABS for UAV

### 2.1 UAV Mathematical Model

The following reasonable assumptions are made when establishing UAV mathematical model:

- Assumption 1: UAV is not affected by side wind during ground taxiing;
- Assumption 2: The friction coefficient of UAV front wheel is a constant;
- Assumption 3: Both sides of the main wheel braking effect is consistent.

Based on the above assumptions, force analysis of fuselage during ground taxiing is shown in Fig. 1.

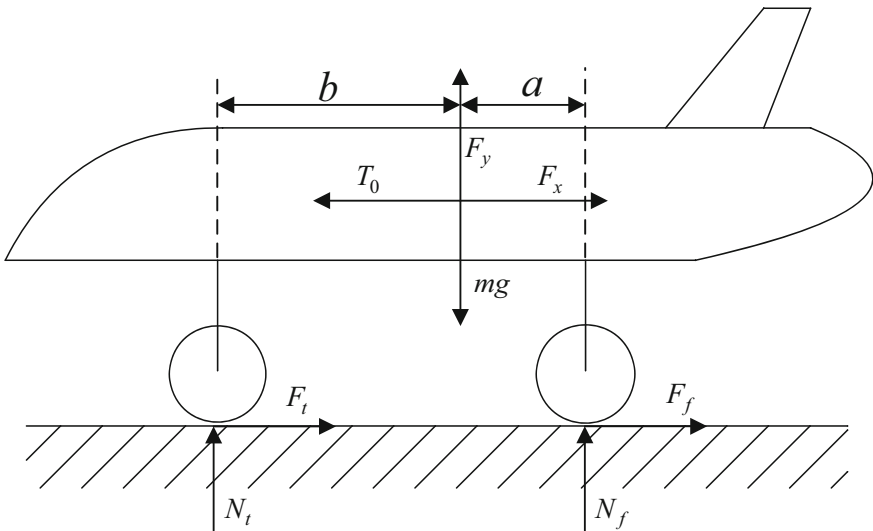


Fig. 1. Analysis of the force on the UAV during ground taxiing.

The model has simple structure but retains the essential characteristics of the braking process, which is suitable for the design of antiskid braking controller of UAV. According

to Newton’s second law of motion, the UAV’s longitudinal motion equation, vertical direction balance equation and centroid moment balance equation can be obtained by Eq. (1):

$$\begin{cases} m\dot{V} + F_x + n_1F_t + n_2F_f - T = 0 \\ mg - F_y - n_1N_t - n_2N_f = 0 \\ n_1N_t b - n_2N_f a - n_2F_f h - n_1F_t h = 0 \end{cases} \quad (1)$$

The aerodynamic drag  $F_x$ , the lift force  $F_y$ , the adhesion between the wheel and the runway  $F_t$  and  $F_f$  can be generated as

$$F_x = \frac{1}{2}JC_xSV^2, F_y = \frac{1}{2}JC_ySV^2, F_t = \mu_f N_t, F_f = \mu N_f \quad (2)$$

where  $m$  is the quality of UAV,  $V$  is the longitudinal sliding speed of the aircraft,  $n_1$  and  $n_2$  are the number of front wheel and main wheel,  $\mu_f$  is the adhesive coefficient between the front wheel and the runway,  $\mu$  is the adhesive coefficient between the main wheel and the runway,  $J$  is air density,  $C_x$  is air resistance coefficient,  $C_y$  is lift coefficient,  $S$  is wing area of UAV,  $T$  is engine thrust,  $g$  is gravitational acceleration,  $a$  is the horizontal distance between the center of gravity of the aircraft and the center of the main wheel,  $b$  is the horizontal distance between the center of gravity of the aircraft and the center of the front wheel, and  $h$  is the distance between the center of gravity of the aircraft and the runway.

The force analysis of the main wheel is shown in Fig. 2.

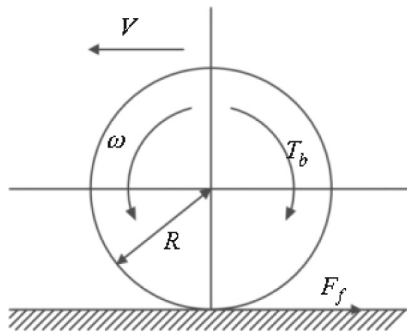


Fig. 2. Analysis of the force on the main wheel

The motion equation of the main wheel during braking can be described as follows:

$$I\dot{\omega} = F_f R - T_b \quad (3)$$

where  $I$  is the rotational inertia,  $\omega$  is angular velocity,  $R$  is wheel radius,  $T_b$  is brake torque.

### 2.2 Slip Ratio Model

The main wheel is applied with braking torque, and the wheel slip ratio reflects the motion characteristics of aircraft during ground taxiing. The slip rate  $\lambda$  can be defined as:

$$\lambda = (V_x - \omega R)/V_x \tag{4}$$

According to UAV mathematical model, the derivative of slip ratio  $\lambda$  is:

$$\dot{\lambda} = -\frac{\mu N_f R^2}{IV} + \frac{1 - \lambda}{mV} (T - F_x - n_2 \mu N_f - n_1 \mu_f N_t) + \frac{R}{VI} T_b \tag{5}$$

To facilitate the later design of the ABS controller, Eq. (5) is expressed as:

$$\dot{\lambda} = f(\lambda) + \frac{R}{IV} T_b \tag{6}$$

where  $f(\lambda) = -\frac{\mu N_f R^2}{IV} + \frac{1 - \lambda}{mV} (T - F_x - n_2 \mu N_f - n_1 \mu_f N_t)$ .

With the aircraft taxiing status and ground conditions changing, the adhesive coefficient is nonlinear variation. In this paper, the Burckhardt model [10, 11] is described as:

$$\mu(\lambda) = [c_1(1 - e^{-c_2\lambda}) - c_3\lambda] e^{-c_4\lambda V} \tag{7}$$

In the formula, the model under different runway states can be established by changing the value  $c_1$ ,  $C_3$ ,  $c_3$  and  $c_4$ . Table 1 lists the values under three different runways.

**Table 1.** Burckhardt model parameters.

Runway states	$c_1$	$c_2$	$c_3$	$c_4$
Dry	1.2801	23.99	0.52	0.04
Wet	0.857	33.822	0.347	0.04
Snow	0.1946	94.129	0.0646	0.04

### 3 Extended State Observer Design

By Considering that there are uncertain disturbances such as parameter perturbation in the anti-skid braking process of UAV and defining  $x_1 = \lambda$ ,  $u = p$ ,  $b_0 = \frac{R}{IV}$ , system (6) can be designed as follows:

$$\dot{x}_1 = f(x_1) + f_d + b_0 u \tag{8}$$

where  $f_d$  represent the uncertain disturbance.

Considering  $f(x_1)$  and  $f_d$  as an extended state and defining  $d = f(x_1) + f_d$ , then system (8) can be described by the following extended state system:

$$\begin{cases} e_z = x_1 - \hat{x}_1 \\ \dot{\hat{x}}_1 = \hat{x}_2 + b_0u + \beta_1e_z \\ \dot{\hat{x}}_2 = \beta_2e_z \end{cases} \tag{9}$$

where  $\hat{x}_1$  and  $\hat{x}_2$  are the estimates of  $x_1$  and  $d$ ,  $e_z$  denotes an estimation error,  $\beta_1$  and  $\beta_2$  are constant gain parameter.

Configure the poles of ESO characteristic equation at the same location, which requires the observer gain to satisfy the following equation:

$$s^2 + \beta_1s + \beta_2 = (s + w_0)^2 \tag{10}$$

where  $w_0$  represent the observer bandwidth. Choosing appropriate  $w_0$  can achieve the precise estimation performance of the designed ESO.

### 4 Controller Design

The control objective of the anti-skid braking system is to ensure that the actual slip rate can track the optimal slip rate, and the slip rate error is defined as  $e = x_1 - \lambda_d$ , so the integral sliding mode surface can be designed as follows:

$$s_p = c \int_0^t edt + e \tag{11}$$

where  $c > 0$  and  $c$  is a constant.

According to sliding function (10) and system (8), the derivative of  $s_p$  is

$$\dot{s}_p = ce + f(x_1) + f_d + b_0u - \dot{\lambda}_d \tag{12}$$

the following reaching law is used to obtain sliding mode control law:

$$u_n = -k_1s_p - \eta sgn(s_p) \tag{13}$$

where  $k_1 > 0$ ,  $\eta > 0$  are reaching law designable parameters.

According to (12) and (13), the control input is constructed as

$$u = -\frac{1}{b_0}(ce + f(x_1) + f_d - \dot{\lambda}_d) - k_1s_p - \eta sgn(s_p) \tag{14}$$

Now, considering the Lyapunov function

$$V_1 = \frac{1}{2}s_p^2 \tag{15}$$

The derivative of  $V_1$  is

$$\dot{V}_1 = -b_0(k_1 s_p^2 + \eta |s_p|) \tag{16}$$

From Eqs. (15) and (16), the complete system is asymptotic.

Due to the unknown disturbance variable  $f_d$  in formula Eq. (14), the output of the controller cannot be obtained directly. Combined with the extended state observer, the control law is designed as follows:

$$u = -\frac{1}{b_0}(ce + \hat{x}_2 - \dot{\lambda}_d) - k_1 s_p - \eta \text{sgn}(s_p) \tag{17}$$

## 5 Simulation Results

To verify the reliability of the designed ABS control law, MATLAB was used for numerical simulation under different working conditions. The initial UAV speed and wheel speed are both 50 m/s, the controller parameters are selected as follows:  $w_0 = 500$ ,  $c = 0.1$ ,  $k_1 = 1500$ ,  $\eta = 0.0001$ . Then, other main simulation parameters are listed in Table 2.

**Table 2.** Main simulation parameters of the UAV model

Name	Value	Name	Value	Name	Value
$m$	860 kg	$n_1$	1	$n_2$	2
$a$	1.34 m	$b$	2.09 m	$h$	0.84 m
$R$	0.25 m	$I$	0.3 kg·m <sup>2</sup>	$g$	9.8 m/s <sup>2</sup>
$J$	1.2 kg/m <sup>3</sup>	$C_x$	0.3 N·s <sup>2</sup> /m <sup>2</sup>	$C_y$	0.6 N·s <sup>2</sup> /m <sup>2</sup>

### 5.1 Ideal Condition

Firstly, the numerical simulation is carried out on a dry runway and a snow runway with low friction coefficient, the simulation results are shown in Fig. 3.

It can be seen from the Fig. 3 that the optimal slip rate of real-time change is well tracked, the adhesive coefficient remains the maximum value of Eq. (7), and the aircraft and the wheel speed decelerate smoothly.

### 5.2 Step Reduction of Braking Torque

The braking torque step of the braking system is reduced by 200 N·m at 6 s to simulate the working condition of the braking efficiency mutation. On a dry runway, the simulation results of ideal and mutation conditions are compared as shown in the Fig. 4.

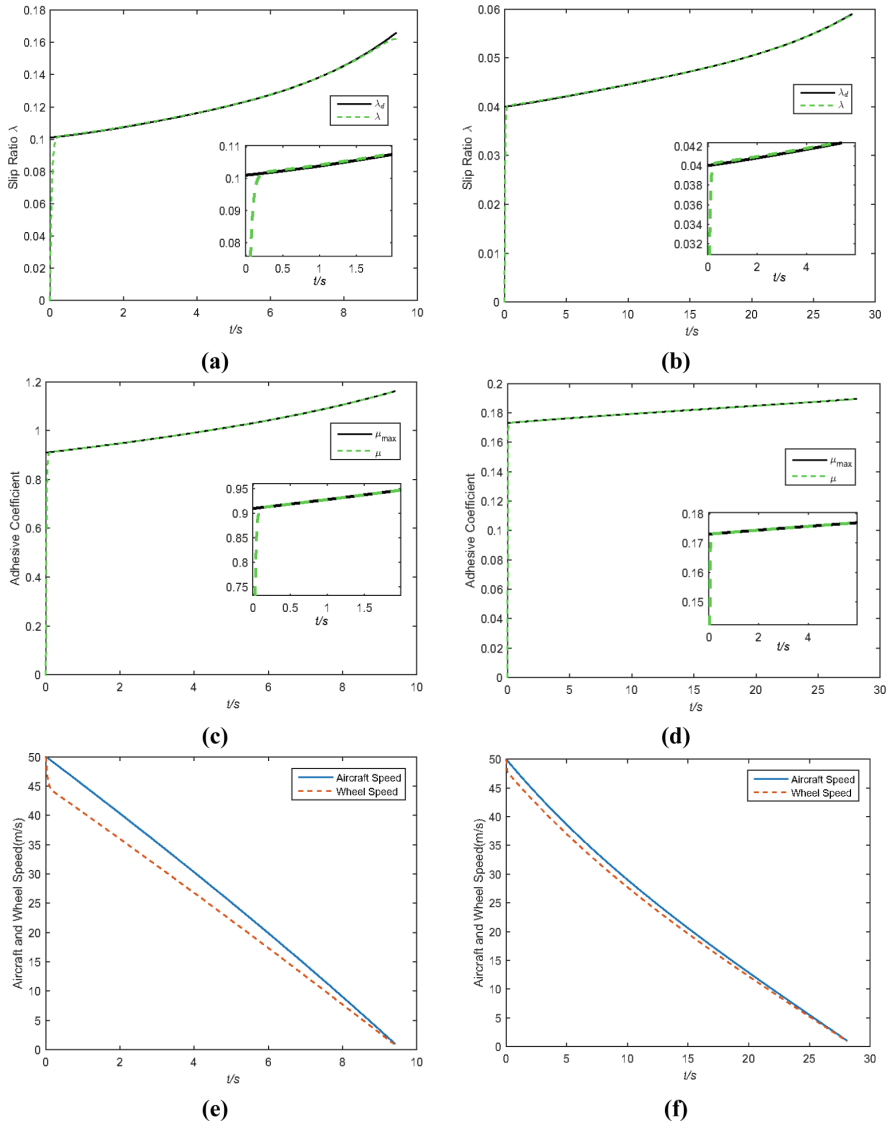


**Fig. 3.** Simulation results of the ABS controller under different runway condition. **a** slip rate under dry runway; **b** slip rate under snow runway; **c** adhesive coefficient under dry runway; **d** adhesive coefficient under snow runway; **e** aircraft and the wheel speed under dry runway; **f** aircraft and the wheel speed under snow runway; **g** brake torque under dry runway; **h** brake torque under snow runway

It can be seen from the Fig. 4 that the braking torque is suddenly reduced by 200 N·m at 6 s, then, the braking torque is quickly compensated, which is basically consistent with the ideal working condition. Besides, the slip rate mutates at 6 s and the real-time

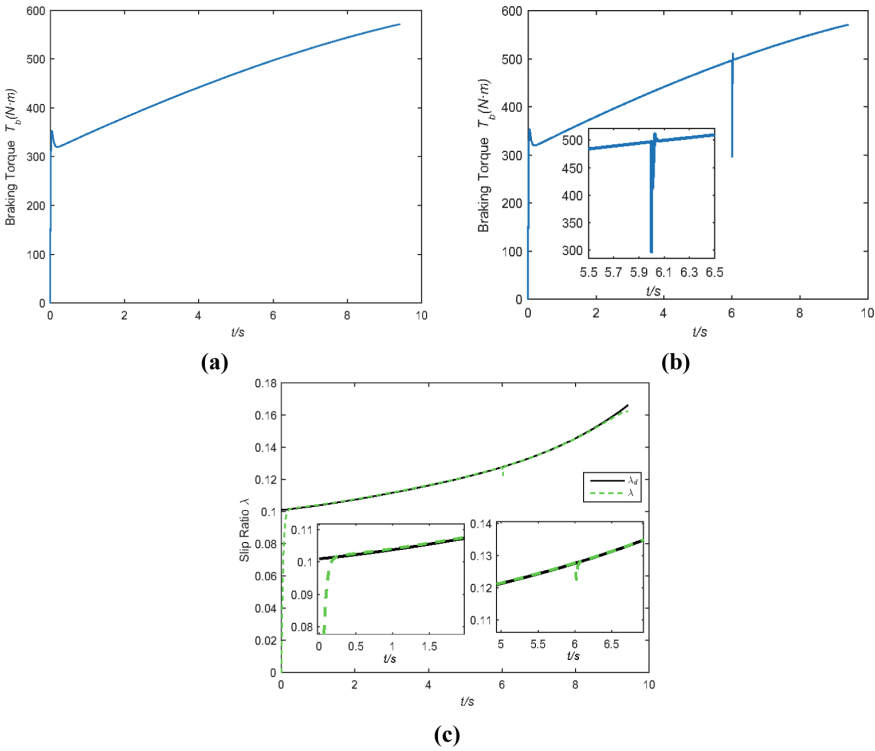


**Fig. 4.** Simulation results of the ABS controller under dry runway condition. **a** braking torque under ideal condition; **b** braking torque under mutation condition; **c** slip rate under mutation condition.

optimal slip rate is well tracked at other times. It is proved that the designed control law can adaptively compensate the disturbance uncertainty caused by input.

### 5.3 Road Changed Suddenly

The numerical simulation is carried out from a dry runway to a wet runway, and this happens at 5s, the simulation results are shown in Fig. 5.

From the Fig. 5, although the road is suddenly changed at 5 s, the real-time optimal slip rate is tracked quickly. This shows that the controller design is adaptable.

### 5.4 Parameter High-Low Bias

To verify the adaptability of the control law to parameter perturbation, considering the deviation range of UAV mass and wheel inertia are both  $\pm 5\%$ , and the maximum negative values are taken in the simulation. On a dry runway, Fig. 6 shows the comparison of simulation results between ISMC based on ESO and ISMC.



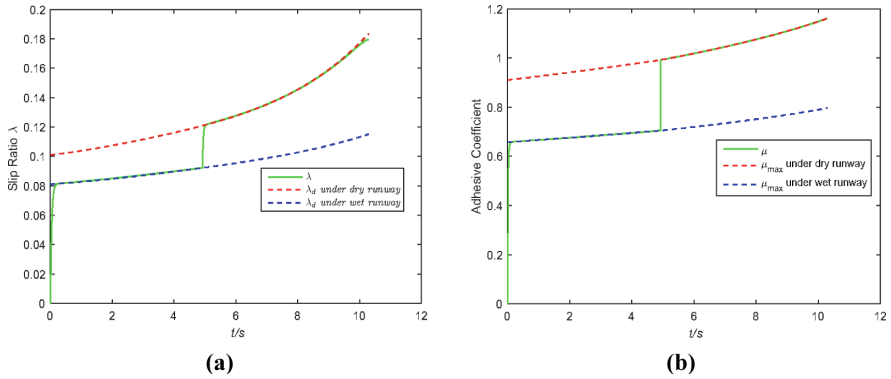


**Fig. 5.** Simulation results of the ABS controller with road changed suddenly. **a** Slip rate; **b** adhesive coefficient

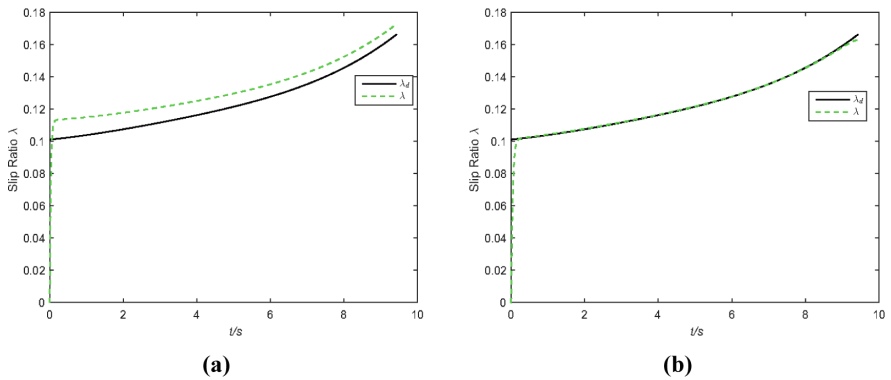


**Fig. 6.** Simulation results of the ABS controller with two control methods under dry runway condition. **a** Slip rate with ISMC; **b** slip rate with ISMC based on ESO.

It can be seen from the Fig. 6 that the optimal slip rate cannot be track only under the action of ISMC in the case of parameter high-low bias, and there is always a steady-state error. The controller with ESO compensation can achieve the control target. It is proved the controller designed has a significant effect on improving the performance of the control system.

## 6 Conclusions

To ensure the safety of take-off and landing of UAV, a new control strategy based on slip ratio is designed. The simulation results show that:

1. This control method can adapt to different runway. When ground taxiing on a dry runway state or a snow runway with low friction coefficient, the real-time optimal slip ratio can be well tracked and the braking efficiency can be improved.

2. The control method has good robustness and high fault tolerance, and can maintain the optimal slip ratio state under different working conditions, including representative road, step reduction of braking torque, road changed suddenly, and parameter high-low bias.

## References

1. Yang, W., Cai, W., Song, Y.: A barrier Lyapunov function (BLF) based approach for antiskid traction/braking control of high speed trains. In: The 26th Chinese Control and Decision Conference (2014 CCDC), pp. 5023–5028. IEEE (2014)
2. Zhang, X., Lin, H.: Backstepping fuzzy sliding mode control for the antiskid braking system of unmanned aerial vehicles. *Electronics* **9**(10), 1731 (2020)
3. Bo, L., Li, Y.: Research on simulation of aircraft electric braking system. In: Recent Advances in Computer Science and Information Engineering, pp. 301–309. Springer, Berlin, Heidelberg (2012)
4. Qiu, Y., Liang, X., Dai, Z.: Backstepping dynamic surface control for an anti-skid braking system. *Control Eng. Pract.* **42**, 140–152 (2015)
5. Ćirović, V., Aleksendrić, D.: Adaptive neuro-fuzzy wheel slip control. *Expert Syst. Appl.* **40**(13), 5197–5209 (2013)
6. Poursamad, A.: Adaptive feedback linearization control of antilock braking systems using neural networks. *Mechatronics* **19**(5), 767–773 (2009)
7. Li, S., Guo, L., Zhang, B., et al.: MPC-based slip control system for in-wheel-motor drive EV. *IFAC-PapersOnLine* **51**(31), 578–582 (2018)
8. Han, J.Q.: From PID technique to active disturbances rejection control technique. *Basic Autom.* (2002)
9. Guermouche, M., Ahmed Ali, S., et al.: An adaptive integral sliding mode control design for internal combustion engine air path. *IFAC Proc. Vol.* **46**(25), 87–94 (2013)
10. Burckhardt, M.: *Fahrwerktechnik: Radschlupfregelsysteme*. Vogel-Verlag, Würzburg (1993). (in German)
11. Baffet, G., Charara, A., et al.: Sideslip angle, lateral tire force and road friction estimation in simulations and experiments. In: Proceedings of the 2006 IEEE International Conference on Control Applications, Munich, Germany, pp. 903–908 (2006)